Elliptical Cavity Resonators for Dual-Mode Narrow-Band Filters

Luciano Accatino, *Member, IEEE,* Giorgio Bertin, *Member, IEEE,* and Mauro Mongiardo, *Member, IEEE*

***Abstract*— A novel cavity resonator with elliptical cross section is proposed in order to realize dual-mode narrow-band filters without tuning and coupling elements. The absence of any discontinuity inside the cavities significantly enhances the unloaded Q, the ability to operate with higher power levels, and the ease of manufacturing. Proper choice of the ellipticity and of the inclination angle controls the desired coupling and tuning actions. Dual-mode coupling is generated by the step discontinuity between the input rectangular waveguide and an inclined elliptical waveguide. A rigorous full-wave electromagnetic model for this discontinuity has been developed and validated using a specialized hardware configuration. Experimental data compare very favorably with theoretical results. Representative prototypes of elliptical cavities exhibiting various degrees of coupling have been carefully measured proving the accuracy of the model and its applicability for narrow-band X- and Ku-band filter design. The full-wave analysis of a complete four-pole narrow-band elliptic filter at 12 GHz and the measured response of a corresponding prototype demonstrate the capability of achieving reliable results using the proposed approach.**

***Index Terms*— Elliptic filters, elliptical waveguide, mode-matching methods.**

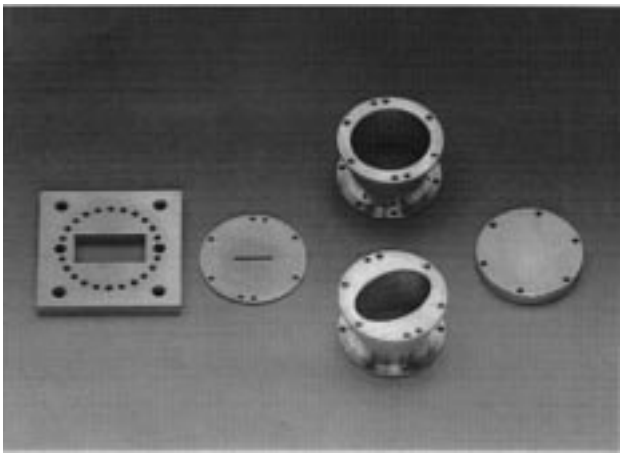

Fig. 1. Photograph of the proposed cavity with elliptical cross section. From left to right: Input rectangular-waveguide flange (WR75), input iris, two test cavities of elliptical cross section, and short circuit. The discontinuity between the rectangular input iris and the inclined elliptical cavity generates the sought mode coupling.

I. Introduction

DUAL-MODE narrow-band filters, since their introduction in the early 1970's [1], are playing a major role in satellite payloads and are still receiving considerable attention for possible improvements. At first, attention was conveyed to the synthesis of transfer functions or to the tuning of actual filter structures [1]–[3]. More recently, however, investigations have been mainly focused on alternative filters structures in order to realize the goal of filter manufacturing directly from a set of physical dimensions as obtained from a computer-aided synthesis algorithm; hence, avoiding any post-manufacturing adjustments.

Several cavities are currently used for dual-mode filters, with relative advantages and disadvantages briefly summarized below. The first cavity structure proposed for dual-mode filters [1] is a standard circular cavity with screws for providing the necessary tuning and coupling actions. The high field concentration near the screws, the modest suitability for CAD representation, and the necessity of post-manufacturing adjustments have stimulated alternative arrangements. Designs which have followed have tried to remove the presence of screws altogether, and solutions for rectangular [4] and circular [5] cavities have been recently presented. However, in both cases there are margins for improvements. The computer-aided design (CAD) of the cavity proposed in [4] suffers from numerical inefficiencies, which owing to the nonseparable nature of the waveguide cross section, poses problems when computing a large numbers of modes, as necessary for narrow-band filters. The circular cavity proposed in [5], though being very suitable for efficient and accurate CAD, presents a discontinuity placed inside the circular cylindrical cavity which causes a degradation of the unloaded Q. Moreover, both solutions [4], [5] exhibit sharp edges within the cavity body; hence, reducing power-handling capabilities.

We consider a new cavity, shown in Fig. 1, which is formed by a length of waveguide with elliptical cross section inclined with respect to the input rectangular waveguide. The latter cavity possesses the following advantages:

- higher power-handling capability, higher unloaded Q;
- ease of manufacturing;
- suitability for CAD modeling.

The first point is achieved since no discontinuities are present inside the cavity. The manufacturing is mainly realized by using milling techniques; finally, efficient and accurate CAD modeling is achieved since the cavity is formed by a guide with separable cross section, i.e., with the spectrum analytically known.

Manuscript received March 31, 1997; revised August 15, 1997.

L. Accatino and G. Bertin are with the Centro Studi e Laboratori, Telecomunicazioni (CSELT), Torino, Italy (e-mail: luciano.accatino@cselt.it; giorgio.bertin@cselt.it).

M. Mongiardo is with Istituto di Elettronica, Università di Perugia, I-06100 Perugia, Italy (e-mail: mongiard@unipg.it).

Publisher Item Identifier S 0018-9480(97)08911-4.

It will be shown in this paper that by properly inclining (see Fig. 1) an elliptical cavity with respect to the input rectangular guide and by suitably selecting the cavity aspect ratio (defined as the ratio between the major and minor axes of the ellipse), it is possible to obtain the desired coupling and tuning actions without introducing any element inside the cavity.[1] In Section II, we present the rigorous analysis of the step discontinuity between the input rectangular waveguide and the elliptical cavity; also discussed is the relative experimental validation of the theoretical model. Dual-mode generation and the operation of the cavity are discussed in Section III; in the same section, a sensitivity analysis is also performed. Section IV considers the intercavity coupling which is preliminary to a filter design. Finally, a theoretical simulation of an entire filter structure is presented and discussed in Section V.

II. The Step Discontinuity Between a Rectangular and an Elliptical Waveguide

A. Theory

The rigorous full-wave characterization of the step discontinuity between waveguides with rectangular and elliptical cross sections play a fundamental role in the design of the proposed cavity for dual-mode filters applications. The above step-discontinuity problem has not appeared in the literature so far; recently, the step discontinuity between two confocal elliptical waveguides has been considered in [7].

In the following, we will refer to a fairly standard scattering formulation of the step discontinuity between two waveguides with different cross sections, as given in [6, eq. (2)–(7)]. In the latter formulation, the transverse components of the electromagnetic field at both sides of the discontinuity are expressed as a modal sum of incident and reflected waves. Continuity of the transverse components of the electric and magnetic fields is imposed on the aperture connecting the two waveguides and the vanishing of the transverse electric field is enforced on the transverse metallic surface surrounding the aperture in the waveguide with larger cross section. For our present purposes of investigating the elliptical-cavity behavior for dual-mode filters applications, we need to consider a junction of enlargement type, i.e., a junction between a smaller rectangular cross section and a larger elliptical waveguide, as shown in Fig. 2. The two-dimensional (2-D) coupling integrals between the modes of the rectangular and elliptical waveguides are transformed into line integrals, which are more appropriate for numerical evaluation by invoking Green's first identity; hence, obtaining the following one-dimensional (1-D) coupling integrals [7, eq. (8)]:

$$A^{\mathrm{TE-TE}}(i,j) = \frac{k_{t_j}^{\mathrm{I}^2}}{k_{t_j}^{\mathrm{I}^2} - k_{t_i}^{\mathrm{II}^2}} \oint_\gamma \Psi_j^{\mathrm{I}} \frac{\partial \Psi_i^{\mathrm{II}}}{\partial n}\, d\ell$$

$$A^{\mathrm{TM-TM}}(i,j) = \frac{k_{t_i}^{\mathrm{II}^2}}{k_{t_i}^{\mathrm{II}^2} - k_{t_j}^{\mathrm{I}^2}} \oint_\gamma \Phi_i^{\mathrm{II}} \frac{\partial \Phi_j^{\mathrm{I}}}{\partial n}\, d\ell$$

$$A^{\mathrm{TE-TM}}(i,j) = \oint_\gamma \Phi_i^{\mathrm{II}} \frac{\partial \Psi_j^{\mathrm{I}}}{\partial s}\, d\ell \qquad (1)$$

[1] Patent pending.

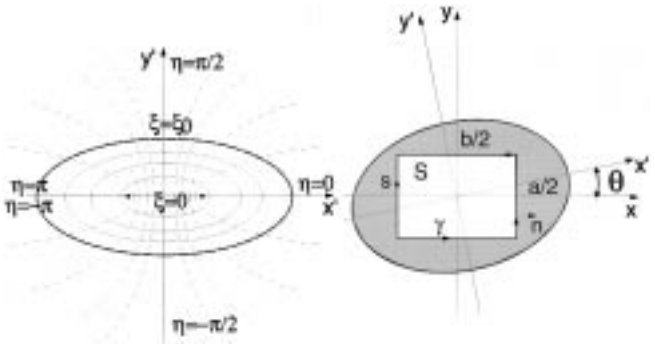

(a) (b)

Fig. 2. (a) Elliptical coordinate system and geometry of the inclined junction between a rectangular waveguide and an (b) elliptical waveguide showing an inclination angle.

where k_t^ν is the modal wavenumber in the rectangular ($\nu = \mathrm{I}$) or elliptical ($\nu = \mathrm{II}$) waveguide, γ is the boundary of S, $\hat{n}$ is the unit vector defined along γ pointing outward from S, and $\hat{s}$ is the unit vector identifying the counterclockwise direction tangent to γ, as depicted in Fig. 2. Φ_i^ν and Ψ_j^ν represent TM and TE potentials, respectively, in the rectangular ($\nu = \mathrm{I}$) or elliptical ($\nu = \mathrm{II}$) waveguide. Note that coupling integral TM–TE is always zero due to the vanishing of the TM eigenfunctions of the rectangular (smaller) waveguide along the integration contour.

For reference purposes the above coupling integrals are detailed in the Appendix, while the expressions of the TE and TM potentials of the elliptical and rectangular waveguides are considered in the following section.

1) Elliptical-Waveguide Potentials: Modes of elliptical waveguides have been studied in [8] and [10] and are briefly summarized below. The wave equation is written in the elliptical coordinates ξ, η, for either TE and TM potentials as

$$\left[\frac{\partial^2}{\partial \xi^2} + \frac{\partial^2}{\partial \eta^2} + 2q(\cosh 2\xi - \cos 2\eta)\right] \begin{Bmatrix} \Psi^{\mathrm{II}} \\ \Phi^{\mathrm{II}} \end{Bmatrix} = 0 \qquad (2)$$

where

$$q = \frac{k_t^{\mathrm{II}^2} h^2}{4}, \qquad h = a_e e \qquad (3)$$

with a_e being the major semiaxis of the ellipse and e representing the ellipticity. TE and TM potentials are obtained by separation of variables of the wave equation which is transformed into the ordinary Mathieu equation and the modified Mathieu equation. The ordinary Mathieu equation is

$$\left[\frac{\partial^2}{\partial \eta^2} + (\alpha - 2q\cos 2\eta)\right] \begin{Bmatrix} ce_m(\eta, q) \\ se_m(\eta, q) \end{Bmatrix} = 0 \qquad (4)$$

with solutions provided by the ordinary even and odd Mathieu functions $ce_m(\eta, q)$ and $se_m(\eta, q)$, respectively. The modified Mathieu equation has the form

$$\left[\frac{\partial^2}{\partial \xi^2} - (\alpha - 2q\cosh 2\xi)\right] \begin{Bmatrix} Ce_m(\xi, q) \\ Se_m(\xi, q) \end{Bmatrix} = 0 \qquad (5)$$

with solutions provided by the modified even and odd Mathieu functions $Ce_m(\xi, q)$ and $Se_m(\xi, q)$, respectively. The parameter α is a separation constant depending on q.

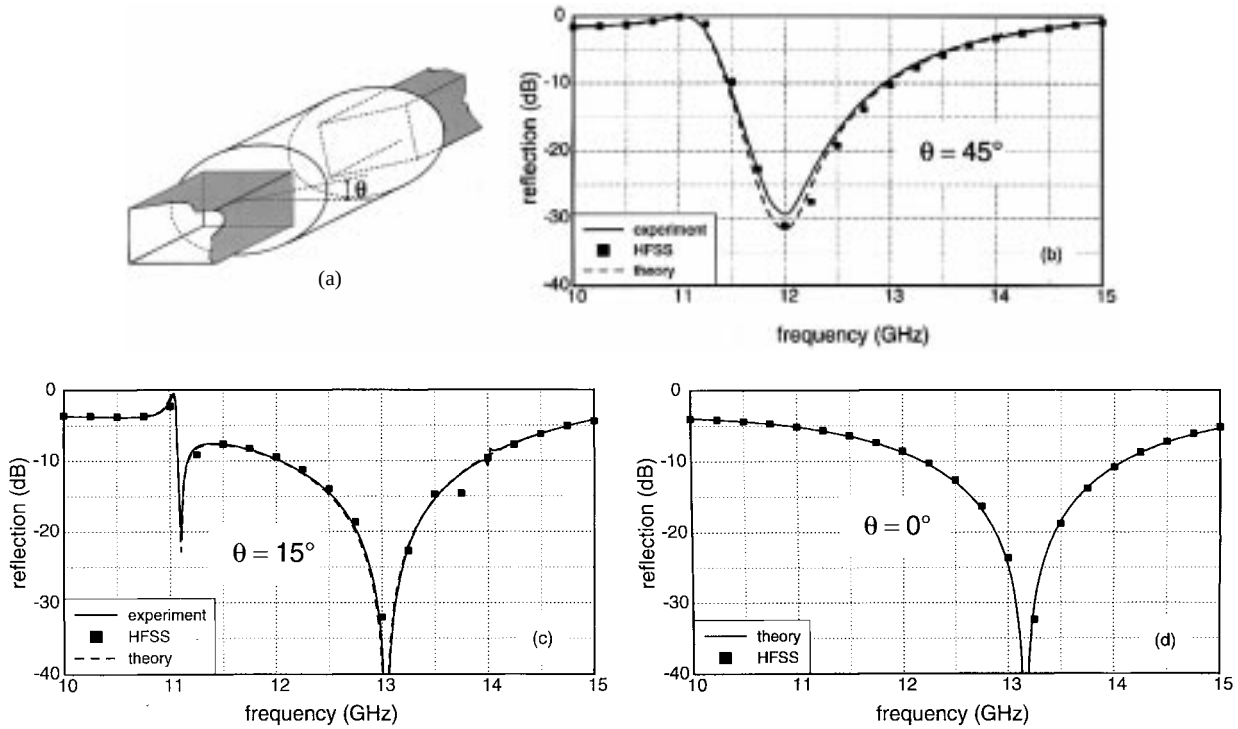

Fig. 3. (a) Outline of back-to-back configuration with two step discontinuities, one of which shows an inclination angle (access guides are WR75, major axis is 22 mm, minor axis is 21.6 mm, and length is 16.5 mm). Plotted for different inclination angles are (b) $\theta = 45^\circ$, (c) 15°, and (d) $\theta = 0^\circ$, respectively, the theoretical results, the experimental data, and the data obtained by using HP HFSS.

The TE and TM potentials are expressed as a combination of the ordinary even and odd Mathieu functions $ce_m(\eta, q)$ and $se_m(\eta, q)$, and of the modified even and odd Mathieu functions $Ce_m(\xi, q)$ and $Se_m(\xi, q)$, respectively, as

$$\begin{Bmatrix} \Psi^{\mathrm{II}} \\ \Phi^{\mathrm{II}} \end{Bmatrix} = \begin{Bmatrix} Ce_m(\xi, q)ce_m(\eta, q) \\ Se_m(\xi, q)se_m(\eta, q) \end{Bmatrix}. \tag{6}$$

Enforcement of boundary conditions on the waveguide walls require

$$\text{TM modes: } Ce_m(\xi_0, q) = 0 \qquad Se_m(\xi_0, q) = 0 \tag{7}$$

$$\text{TE modes: } Ce'_m(\xi_0, q) = 0 \qquad Se'_m(\xi_0, q) = 0 \tag{8}$$

with the prime denoting the derivative and ξ_0 the position of the metallic boundary. It is noted that for each root of (7) and (8) we get a different mode, i.e., a value of q and, by (3), a different value of k_t^{II}. Hence, there are four types of propagation in an elliptical waveguide, namely, even and odd TE and TM modes.

2) Rectangular-Waveguide Potentials: With the adopted coordinate system (see Fig. 2), we have the following expressions for TE and TM potentials:

$$\Psi^{\mathrm{I}}_{m,p}(x, y) = \cos\left[k_x\left(x + \frac{a}{2}\right)\right]\cos\left[k_y\left(y + \frac{b}{2}\right)\right]$$

$$\Phi^{\mathrm{I}}_{m,p}(x, y) = \sin\left[k_x\left(x + \frac{a}{2}\right)\right]\sin\left[k_y\left(y + \frac{b}{2}\right)\right] \tag{9}$$

with k_x and k_y defined as

$$k_x = \frac{m\pi}{a}; \quad k_y = \frac{p\pi}{b}. \tag{10}$$

B. Numerical Computations and Experimental Validation of the Rectangular–Elliptical Step Discontinuity

The spectrum computation of elliptical waveguides has received considerable attention in the past [8], [10], [11]; more recently, interest has again been raised [12]–[15]. It is noted, however, that for narrow-band filter applications, a considerable accuracy is required; moreover, for typical cases, the algorithm should be able to provide a fairly large number of modes (several hundreds TE and TM modes for the accurate analysis of the step discontinuity).

Numerical calculations start with the computation of separation constants (4), (5), also known as "characteristic values" of Mathieu functions, and carried out according to the algorithm reported in [11]. Ordinary expansion of Mathieu functions is in terms of trigonometric and exponential functions [8, ch. 2], but this expansion has a rather poor convergence radius and fails to give accurate results when the argument or the order are just moderately large.

A more efficient expansion that has actually been used in our calculations, is in terms of Bessel functions [8, ch. 8]. In addition to being numerically much more stable, this expansion has (in our case of moderate elliptical shape) the further advantage of highlighting similarities and deviations with respect to the circular guide. Numerical computation schemes are worked out according to [8, ch. 8] and [9, ch. 20] and give accurate results up to large values of arguments and orders.

Since no experimental data are available for the junction between a rectangular and an elliptical waveguide, we have built and measured a structure with two step discontinuities

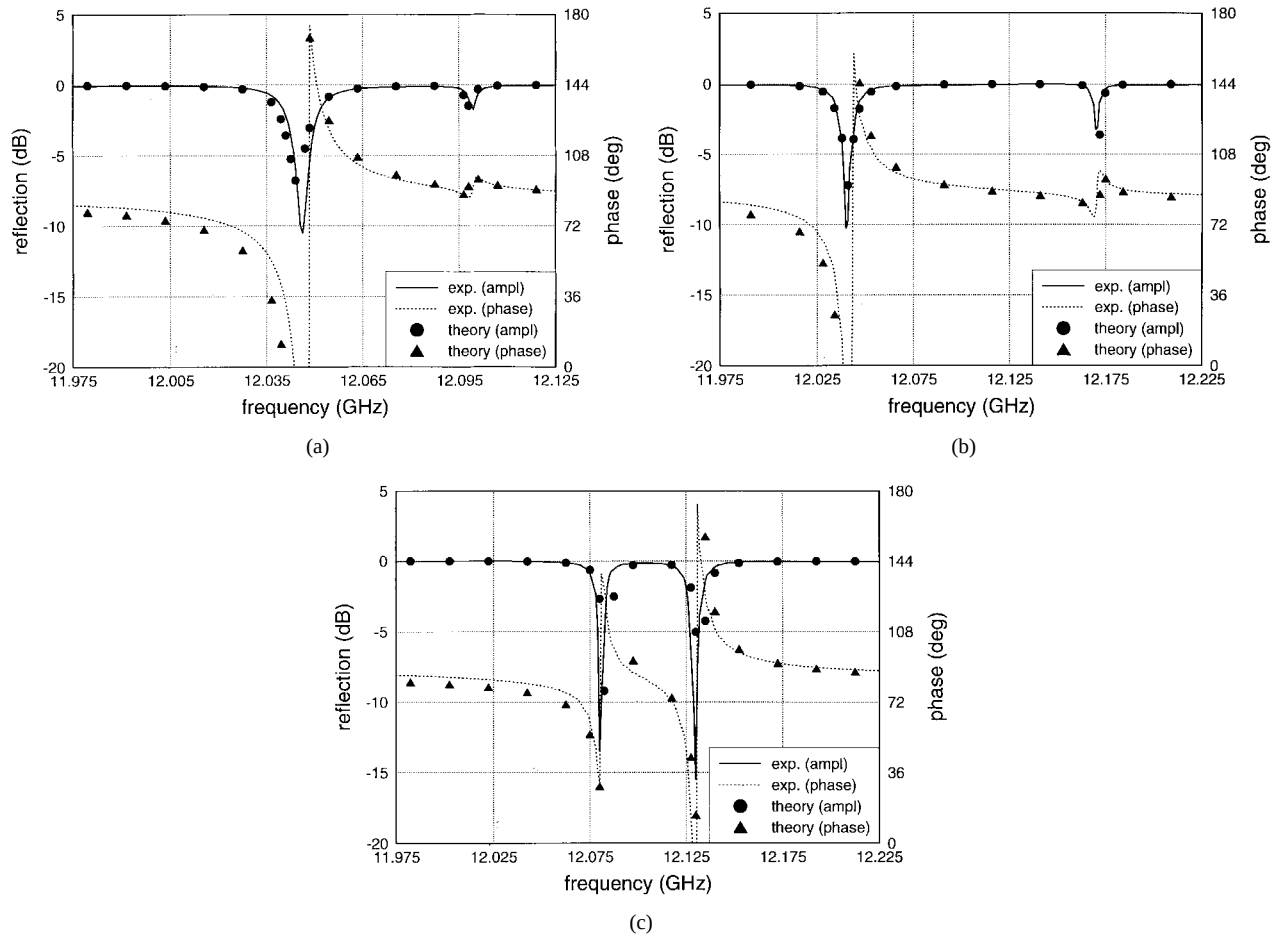

Fig. 4. Reflection coefficient of the short-circuited cavity shown in Fig. 1. The feeding waveguide is a WR 75 and the input iris dimensions are 8-mm wide, 0.75-mm high, and 1-mm thick. The major axis of the elliptical cavity is 22 mm and the minor axes and inclinations are as follows. (a) Minor axis is 21.9 mm, $\theta = 60^\circ$. (b) Minor axis is 21.6 mm, $\theta = 30^\circ$. (c) Minor axis is 21.6 mm, $\theta = 75^\circ$.

placed back-to-back. This configuration, having equal access guides, makes measurements easier. Moreover, since the output step is allowed to show an inclination angle with respect to input guide, this feature is also fully validated. The geometry of the step discontinuities is shown in Fig. 3(a) and related dimensions are given in the caption.

It is noted that very good agreement is present between modal analysis and the experimental data. The theoretical results generated with modal analysis have employed 20 TE and 14 TM modes in the rectangular waveguides and 37 TE and 25 TM modes in the elliptical waveguide; computation time for 100 frequency points is approximately 63 s on an HP 735 workstation. Also noted is the good agreement with HP HFSS, which apart for one point in Fig. 3(c), provide a fairly accurate result. However, the FEM adopted in HFSS is not the most efficient approach for waveguiding problems; in fact, computation of 21 frequency points requires approximately 2 h. The latter figures make clear that the HFSS represents an excellent and versatile tool for code or structure validation, but is not particularly suitable for efficient filter design.

III. Dual-Mode Operation

From a more detailed observation of the resonances present in Fig. 3(c) it is also apparent that the inclined junction between the rectangular and elliptical waveguide is able to produce the dual polarization. In Fig. 3(d), where the inclination angle θ is zero, we have just one resonant mode inside the cavity; however, when a certain inclination angle is considered, e.g., $\theta = 15^\circ$ as in Fig. 3(c), we note two resonant modes being present inside the cavity. Finally, in Fig. 3(b), the two resonances merge together, thus showing just an enlarged one. This behavior is investigated more carefully by considering the short-circuited cavity.

A. The Short-Circuited Cavity

Cavity aspect ratios suitable for a dual-mode application are those close to the circular shape, since it is to be expected that a small shrinking of the minor axis of the ellipse is sufficient to produce the desired coupling action [5].

In particular, two aspect ratios have been tested under a moderately large input coupling sufficient to overcouple the resonators in order to get a significant response both in amplitude and in phase. Cross sections of both cavities have a major axis of 22 mm, minor axis of 21.9 mm for cavity one (the corresponding aspect ratio being 1.004 566), and 21.6 for cavity two (aspect ratio 1.018 52). All cavities have been measured in the range of inclinations from 0° to 90° with a step of 15°; precision alignment p-i-n's have been used

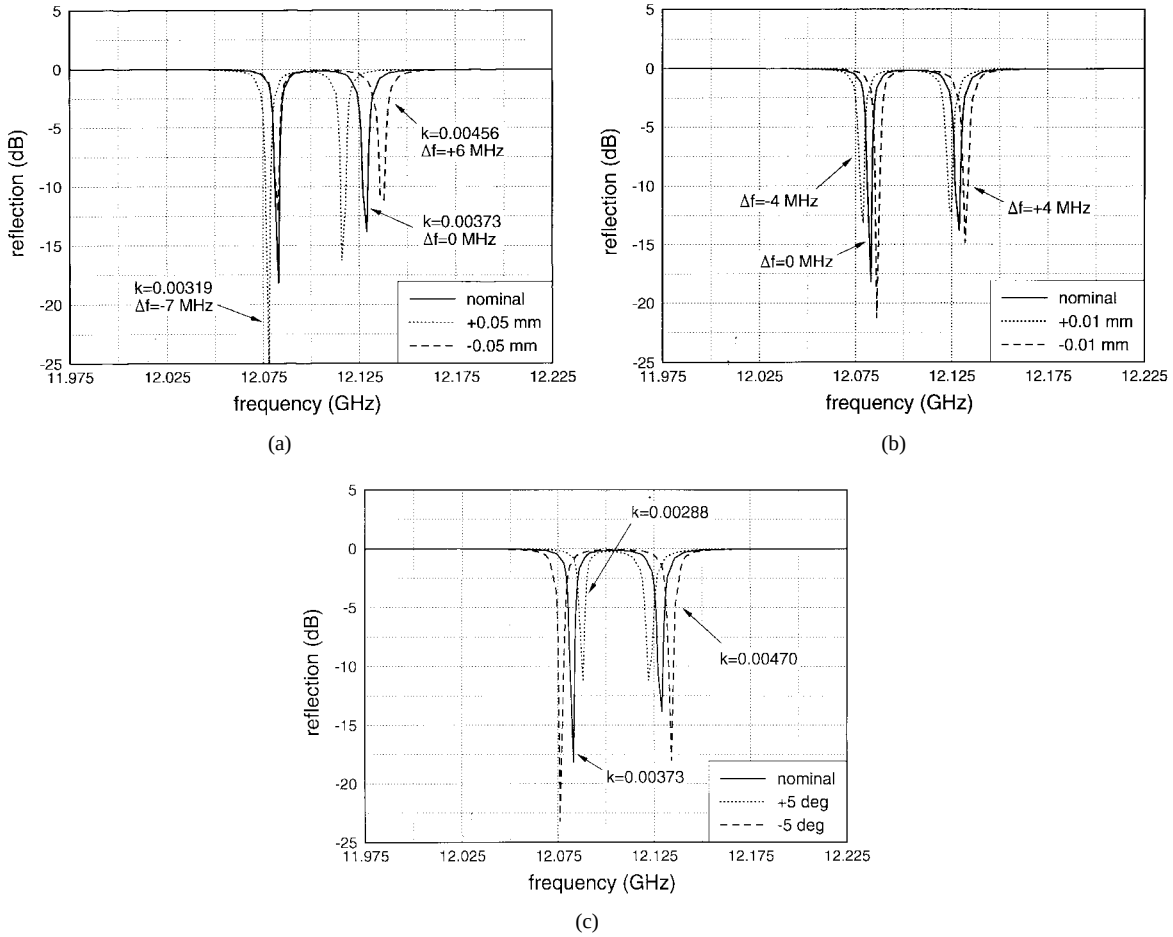

Fig. 5. (a) Sensitivity analysis of the short-circuited cavity with respect to variations of the ellipticity of (b) the cavity length and (c) the inclination.

in order to ensure close control of the setup under measurement. Representative data are reported in Fig. 4(a)–(c), where measured responses are also compared with mode-matching simulations. In particular, Fig. 4(a) shows cavity one with an inclination of 60°. We may note that a very good agreement is maintained even for this aspect ratio and that being close to the circular shape requires a fairly lengthy and time-consuming mode search for the elliptic guide. Cavity two is shown for two angular positions of 30° [Fig. 4(b)] and 75° [Fig. 4(c)], respectively. Apart from the good agreement between theory and experiment, it is interesting to observe the situation of Fig. 4(c), where the depth of the two resonant peaks is approximately equal. It is well known that this corresponds to a synchronous tuning of the two resonant modes. In other words, measured data show the response of a tuned dual-mode cavity in which the reactive loading of the input iris has been perfectly compensated, as explained in [18]. This further proves the tuning and coupling capability of the new cavity.

B. Sensitivity Analysis

The nearly tuned configuration reported in Fig. 4(c) has been taken as a reference for some representative sensitivity calculations. The aim of these computed data is to provide a better insight into the allowed tolerance to be sought for the mechanical realization of the proposed new filter structure. Moreover, by choosing a tuned configuration it is possible to deduce, in addition to data concerning the response deviation from the reference condition, data relative to equivalent coupling coefficients—the latter being particularly significant for filter applications.

In particular, a variation of $\pm$ 0.01 mm in the cavity length, of $\pm$ 5° in the inclination, and of $\pm$0.25% in the aspect ratio (corresponding to approximately $\pm$ 0.05 mm in the minor axis), has been applied. The results are shown in Fig. 5 where, in all cases, the solid line represents the reference condition and the dashed lines the variations.

As can be seen, in case Fig. 5(b) (variation in length) the result is a bare shift of the response of approximately 4 MHz, with a coupling coefficient that remains virtually unchanged. In the case of a four-pole filter (two cavities) this would correspond to a shift in frequency of the response with a negligible degradation of the shape. A variation in inclination [see Fig. 5(c)] produces, on the contrary, appreciable effects only on the coupling coefficient, leaving the center frequency nearly unaffected. It can be inferred from the data shown that to keep the coupling error within $\pm$ 1% the allowed error in the inclination angle is 0.2%. Finally, a variation in the aspect ratio (that is one or both of the ellipse axes) produces a simultaneous coupling and detuning error [see Fig. 5(a)]. This makes this kind of variation the most critical. Data worked out from the curve shown give a permissible error of $\pm$ 0.005

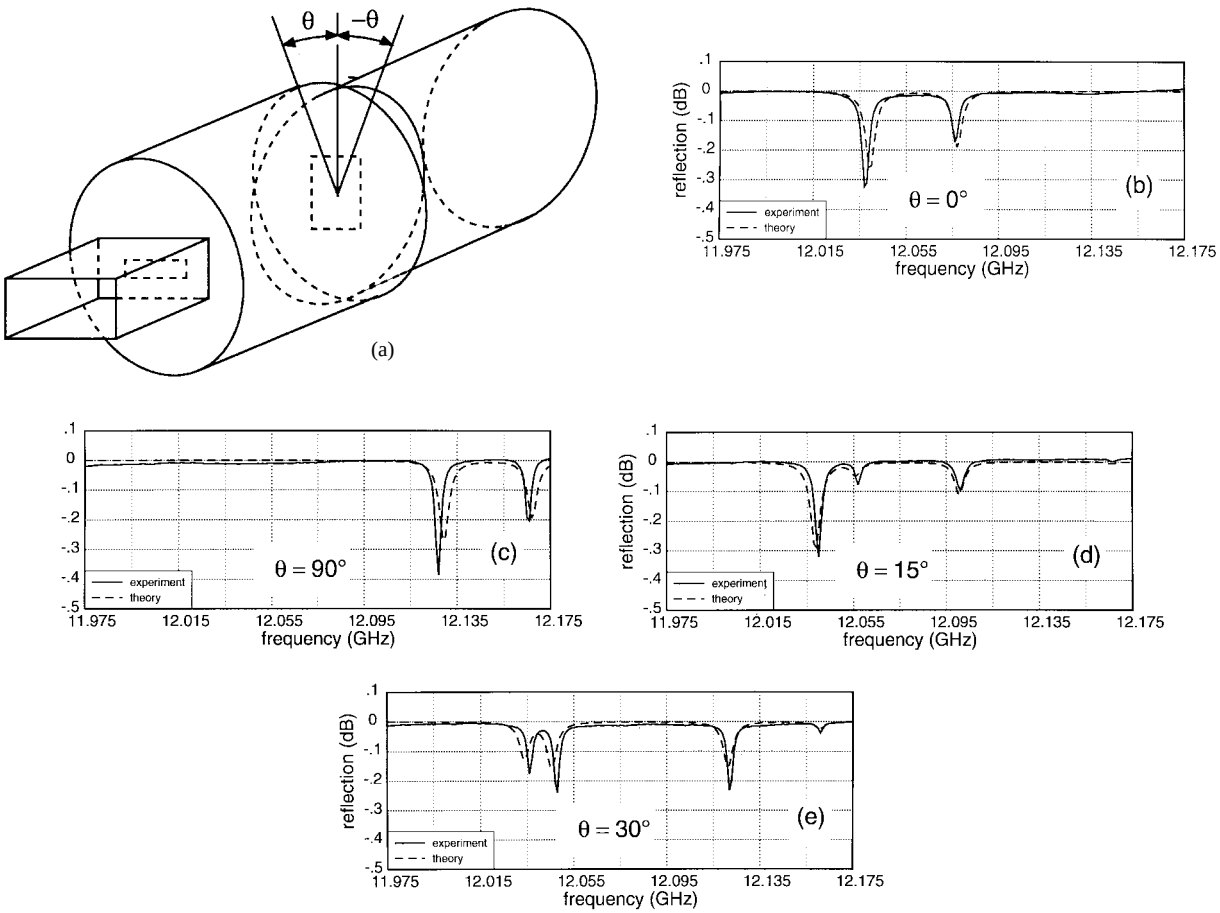

Fig. 6. (a) Sketch of the intercavity geometry. Note that the two elliptical cavities are oriented in opposite directions. Intercavity coupling for different inclination angles of the elliptical cavities in (b) $\theta = 0^\circ$, (c) $\theta = 90^\circ$, (d) $\theta = 15^\circ$, and (e) $\theta = 30^\circ$. The dimensions of the intercavity iris are 3.78-mm wide, 5.31-mm high, and 1-mm thick. The major axis of the elliptical cavities is 22 mm, the minor axis 21.6, and their length is 16.5 mm. The feeding rectangular waveguide is a WR75 and the input iris dimensions are 5-mm wide, 0.5-mm high, and 1-mm thick.

mm in order to maintain coupling and detuning errors within acceptable margins.

IV. Study of Intercavity Coupling

The dual-mode cavity examined in details in the two previous sections is the basic building block of a dual-mode filter. A second key element that deserves considerable attention before proceeding to the design and fabrication of an entire filter structure is the coupling between adjacent cavities that is accomplished by inserting a rectangular aperture in the common wall between the two resonators with elliptical cross section. The accuracy of the rectangular-to-elliptical scattering described in Section II has been tested also in this configuration, especially with reference to the case of the two cavities with opposite inclinations, since the latter configuration typically occurs in the design of filters having finite-transmission zeros.

The two cavities under test [Fig. 6(a)] have been aligned at first, either with the major axis placed horizontally (case b) or vertically (case c). In both cases, a very good agreement between measured and theoretical data can be observed. Moreover, since the variation of the coupling coefficient is quite modest between these limiting cases, it can be reasonably argued that there is a very weak dependence of the intercavity coupling with respect to inclination, this information being particularly useful for design purposes. However, in order to provide a further check of the developed theory, the configuration with the cavities showing an opposite inclination, either of $\pm$ 15° (case d) and $\pm$ 30° (case e) have also been considered. As it is expected, when the two cavities are not aligned all four resonant modes (two in each dual-mode cavity) are excited and are visible in the input reflection response, as is shown in the two cases considered. The correlation between the computed and measured responses is again very good, proving the accuracy and the reliability of the simulation tools that have been developed for elliptical cavities.

V. Discussion

A. Ease of Manufacturing

Several prototypes of elliptic cavities with different aspect ratios have been machined out of aluminum. The lack of discontinuities inside the cavities has enabled the use of a numerically controlled milling machine. Electric discharge erosion has been limited to input coupling irises, resulting in a potential cost-reducing technology. In particular, good internal surface finish (which has a direct impact on the cavity loss)

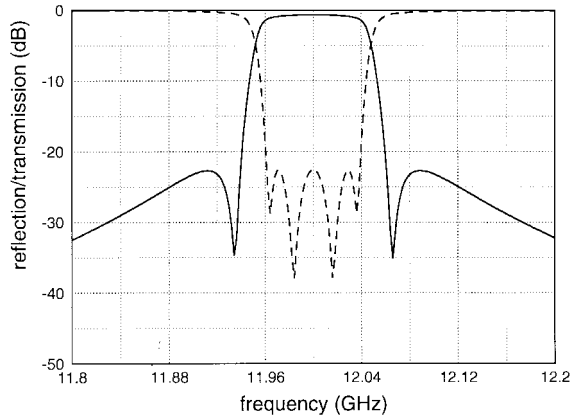

Fig. 7. Computed response of the four-pole elliptic filter.

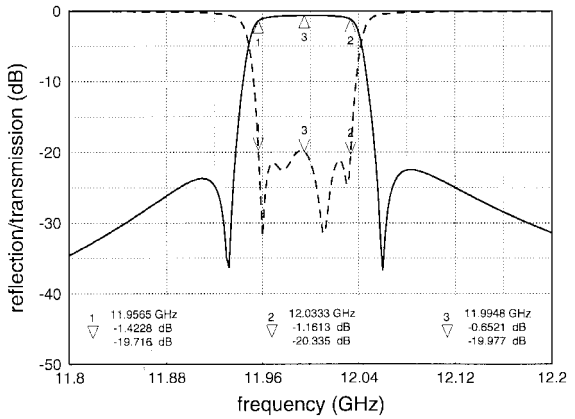

Fig. 8. Measured response of the four-pole elliptic filter (input iris: 9.91 mm × 2.00 mm, thickness 2 mm, cavity: major axis 22.00 mm, minor axis 21.00, length 16.62 mm, inclination 81.46°, central iris: 3.50 mm × 4.98 mm, thickness 1 mm, input/output guide: WR 75).

can be achieved with a substantial cost reduction with respect to a fabrication involving heavy electric-discharge steps.

B. Unloaded Q

The cross-section uniformity also plays an important role in this case. All cavity samples were made using aluminum alloy 7075 T6, which displays a typical conductivity rated at 30%–35% of that of annealed copper. A simple calculation performed according to [16, Ch. 4] for a circular cavity having approximately the same cross section, and with a practical efficiency of 58%, deduced from [17], gives an unloaded Q value slightly less than 4000 at 12 GHz. Measured Q's of elliptic cavities are all in the range of 3700–3800, quite close to the theoretical prediction. Note that these values are nearly 50% higher than those measured in [5], and 25% higher than that of a comparable rectangular cavity.

C. Four-Pole Filter Design and Realization

By extending the mode-matching software developed for a single dual-mode cavity analysis to a full four-pole structure (two cavities), a demonstration filter has been designed. The selected prototype is of an elliptic type (two finite-transmission zeros), has a center frequency of 12 GHz with a passband of 78 MHz and sidelobes of 22.5 dB. Pretuning techniques described in [3] have been extensively employed to obtain a good starting point. A subsequent final optimization has led to the result shown in Fig. 7. The inclination angle of the second cavity is obviously the opposite with respect to the vertical axis of the first one. As can be noted, the typical capability of generating responses with finite zeros of conventional dual-mode filters is fully maintained. The equivalent cavity loss used in computations corresponds to an unloaded Q of 3700.

Starting from the optimized geometrical dimensions, an experimental aluminum prototype has been manufactured (accuracy $\pm$ 0.01 mm) and tested. The measured response reported in Fig. 8 shows good agreement with theoretical computations. In particular, the measured passband and center frequency are very close to theory (difference in bandwidth and frequency is less than 2% and approximately 5 MHz, respectively). The measured return loss exceeds 20 dB and out-of-band sidelobe asymmetries are less than 2 dB.

VI. Conclusion

A novel cavity structure without screws for dual-mode narrow-band filters has been presented which significantly improves the unloaded Q, the ability to operate with high power levels, and the ease of manufacturing. The cavity has elliptical cross section and no tuning or coupling elements are present in its interior; hence, allowing manufacturing by milling techniques. Appropriate tuning and coupling actions are obtained by suitably selecting the inclination angle with respect to the input rectangular waveguide and the ellipticity of the cavity.

A rigorous full-wave electromagnetic model for the step discontinuity between rectangular and elliptical waveguides has been developed and experimentally validated. Measured and theoretical results for different inclination angles and different values of ellipticity of the cavity have been presented, showing the accuracy of the electromagnetic analysis and the validity of the proposed cavity for dual-mode filters applications.

A complete four-pole elliptic filter with center frequency of 12 GHz, a passband of 78 MHz, and sidelobes of 22.5 dB has been designed, manufactured, and tested. Measured response compares favorably with computation and proves the feasibility of the proposed approach in designing and realizing narrow-band bandpass filters without screws and displaying a near-optimum performance in terms of unloaded Q and power-handling capabilities.

Appendix

In order to write the coupling integrals in compact form it is convenient to introduce the following notation:

$$U_m(\xi,\eta) = \begin{Bmatrix} Ce_m(\xi,q)ce_m(\eta,q) \\ Se_m(\xi,q)se_m(\eta,q) \end{Bmatrix}$$
$$V_m(\xi,\eta) = \begin{Bmatrix} Ce'_m(\xi,q)ce_m(\eta,q) \\ Se'_m(\xi,q)se_m(\eta,q) \end{Bmatrix}$$
$$W_m(\xi,\eta) = \begin{Bmatrix} Ce_m(\xi,q)ce'_m(\eta,q) \\ Se_m(\xi,q)se'_m(\eta,q) \end{Bmatrix} \quad (11)$$

where the functions U_m, V_m, and W_m take the even or odd expressions depending on the case considered. It is also expedient to define the functions F_m and G_m as

$$F_m(\xi,\eta) = \left[V_m(\xi,\eta)\frac{\partial\xi}{\partial x} + W_m(\xi,\eta)\frac{\partial\eta}{\partial x}\right]$$
$$G_m(\xi,\eta) = \left[V_m(\xi,\eta)\frac{\partial\xi}{\partial y} + W_m(\xi,\eta)\frac{\partial\eta}{\partial y}\right]. \quad (12)$$

With reference to Fig. 2, the terms $\frac{\partial\xi}{\partial x}$, $\frac{\partial\eta}{\partial x}$, $\frac{\partial\xi}{\partial y}$, and $\frac{\partial\eta}{\partial y}$ are obtained as

$$\frac{\partial\xi}{\partial x} = \frac{h}{\Delta}[\sinh\xi\cos\eta\cos\theta - \cosh\xi\sin\eta\sin\theta]$$
$$\frac{\partial\eta}{\partial x} = \frac{h}{\Delta}[-\cosh\xi\sin\eta\cos\theta - \sinh\xi\cos\eta\sin\theta]$$
$$\frac{\partial\xi}{\partial y} = \frac{h}{\Delta}[\sinh\xi\cos\eta\sin\theta + \cosh\xi\sin\eta\cos\theta]$$
$$\frac{\partial\xi}{\partial y} = \frac{h}{\Delta}[-\cosh\xi\sin\eta\sin\theta + \sinh\xi\cos\eta\cos\theta] \quad (13)$$

with Δ being defined as

$$\Delta = \frac{h^2}{2}(\cosh 2\xi - \cos 2\eta). \quad (14)$$

By expressing ξ and η in terms of x and y, as $\xi + i\eta = \cosh^{-1}(\frac{x+iy}{h})$, we are now in a position to numerically evaluate the coupling integrals between elliptical and rectangular waveguides. For the sake of clarity, we denote with a tilde the functions expressed in terms of the x- and y-coordinates as $\tilde{F}_m(x,y) = F_m(\xi,\eta)$. We also note that by taking advantage of the symmetries, only half of the contour has to be considered when evaluating the coupling integrals.

A. TE–TE Coupling Integrals

For TE–TE coupling we have

$$\oint_\gamma \Psi_j^{\mathrm{I}}\frac{\partial\Psi_i^{\mathrm{II}}}{\partial n}\,d\ell = 2\{I_x + I_y\}$$

with the integrals at constant x, I_x, and y, I_y, respectively, given by

$$I_x = \int_{-b/2}^{b/2}\Psi_j^{\mathrm{I}}\frac{\partial\Psi_i^{\mathrm{II}}}{\partial x}\,dy$$
$$= \cos m\pi\int_{-b/2}^{b/2}\cos\left[k_y\left(y+\frac{b}{2}\right)\right]\tilde{F}_m(x=a/2,y)\,dy$$
$$I_y = \int_{-a/2}^{a/2}\Psi_j^{\mathrm{I}}\frac{\partial\Psi_i^{\mathrm{II}}}{\partial y}\,dx$$
$$= \cos p\pi\int_{-a/2}^{a/2}\cos\left[k_x\left(x+\frac{a}{2}\right)\right]\tilde{G}_m(x,y=b/2)\,dx.$$

B. TM–TM Coupling Integrals

With the above definitions, the TM–TM coupling integrals may be expressed as

$$\oint_\gamma \Phi_i^{\mathrm{II}}\frac{\partial\Phi_j^{\mathrm{I}}}{\partial n}\,d\ell = 2\{I_x + I_y\}$$

with the integrals I_x and I_y now taking the forms

$$I_x = \int_{-b/2}^{b/2}\Phi_i^{\mathrm{II}}\frac{\partial\Phi_j^{\mathrm{I}}}{\partial x}\,dy$$
$$= k_x\cos m\pi\int_{-b/2}^{b/2}\sin\left[k_y\left(y+\frac{b}{2}\right)\right]\tilde{U}_m(x=a/2,y)\,dy$$
$$I_y = \int_{-a/2}^{a/2}\Phi_i^{\mathrm{II}}\frac{\partial\Phi_j^{\mathrm{I}}}{\partial y}\,dx$$
$$= k_y\cos p\pi\int_{-a/2}^{a/2}\sin\left[k_x\left(x+\frac{a}{2}\right)\right]\tilde{U}_m(x,y=b/2)\,dx.$$

C. TE–TM Coupling Integrals

The TE–TM coupling integrals are given by

$$\oint_\gamma \Phi_i^{\mathrm{II}}\frac{\partial\Psi_j^{\mathrm{I}}}{\partial n}\,d\ell = 2\{I_x + I_y\}$$

with the integrals I_x and I_y assuming the meanings

$$I_x = \int_{-b/2}^{b/2}\Phi_i^{\mathrm{II}}\frac{\partial\Psi_j^{\mathrm{I}}}{\partial x}\,dy$$
$$= -k_y\cos m\pi\int_{-b/2}^{b/2}\sin\left[k_y\left(y+\frac{b}{2}\right)\right]\tilde{U}_m(x=a/2,y)\,dy$$
$$I_y = \int_{-a/2}^{a/2}\Phi_i^{\mathrm{II}}\frac{\partial\Psi_j^{\mathrm{I}}}{\partial y}\,dx$$
$$= k_x\cos p\pi\int_{-a/2}^{a/2}\sin\left[k_x\left(x+\frac{a}{2}\right)\right]\tilde{U}_m(x,y=b/2)\,dx.$$

REFERENCES

[1] A. E. Atia and A. E. Williams, "Narrow bandpass waveguide filters," *IEEE Trans. Microwave Theory Tech.*, vol. MTT-20, pp. 258–265, Apr. 1972.

[2] A. E. Williams, R. G. Egri, and R. R. Johnson, "Automatic measurement of filter coupling parameters," in *IEEE MTT-S Int. Symp. Dig.*, Boston, MA, May 1983, pp. 418–420.

[3] L. Accatino, "Computer-aided tuning of microwave filters," in *IEEE MTT-S Int. Symp. Dig.*, Baltimore, MD, June 1986, pp. 249–252.

[4] X.-P. Liang, K. A. Zaki, and A. E. Atia, "Dual mode coupling by square corner cut in resonators and filters," *IEEE Trans. Microwave Theory Tech.*, vol. 40, pp. 2294–2302, Dec. 1992.

[5] L. Accatino, G. Bertin, and M. Mongiardo, "A four-pole dual mode elliptic filter realized in circular cavity without screws," *IEEE Trans. Microwave Theory Tech.*, vol. 44, pp. 2680–2687, Dec. 1996.

[6] L. Accatino and G. Bertin, "Design of coupling irises between circular cavities by modal analysis," *IEEE Trans. Microwave Theory Tech.*, vol. 42, pp. 1307–1313, July 1994.

[7] P. Matras, R. Bunger, and F. Arndt, "Mode-matching analysis of the step discontinuity in elliptical waveguides," *IEEE Microwave Guided Wave Lett.*, vol. 6, pp. 143–145, Mar. 1996.

[8] N. W. McLachlan, *Theory and Application of Mathieu Functions.* New York: Dover, 1974.

[9] M. Abramowitz and I. Stegun, *Handbook of Mathematical Functions*. New York: Dover, 1968, pp. 721–750.

[10] J. G. Kretzschmar, "Wave propagation in hollow conducting elliptical waveguides," *IEEE Trans. Microwave Theory Tech.*, vol. MTT-18, pp. 547–554, Sept. 1970.

[11] W. R. Leeb, "Characteristic values of Mathieu differential equation," *ACM Trans. Math. Software*, vol. 5, pp. 112–117, Mar. 1979.

[12] D. A. Goldberg, L. J. Laslett, and R. A. Rimmer, "Modes of elliptical waveguides: A correction," *IEEE Trans. Microwave Theory Tech.*, vol. 38, pp. 1603–1608, Dec. 1990.

[13] B. K. Wang, K. Y. Lam, M. S. Leong, and P. S. Kooi, "Elliptical waveguide analysis using improved polynomial approximation," *Proc. Inst. Elec. Eng.*, vol. 141, pt. H, pp. 483–488, Dec. 1994.

[14] F. A. Alhargan and S. R. Judah, "Tables of normalized cutoff wavenumbers of elliptic cross section resonators," *IEEE Trans. Microwave Theory Tech.*, vol. 42, pp. 333–338, Feb. 1994.
[15] S. Zhang and Y. Shen, "Eigenmode sequence for an elliptical waveguide arbitrary ellipticity," *IEEE Trans. Microwave Theory Tech.*, vol. 43, pp. 227–230, Jan. 1995.
[16] G. L. Matthaei, L. Young, and E. M. T. Jones, *Microwave Filters, Impedance-Matching Networks, and Coupling Structures*. New York: McGraw-Hill, 1964.
[17] C. M. Kudsia *et al.*, "Status of filter and multiplexer technology in the 12 GHz frequency band for space application," in *Proc. AIAA Conf.*, San Diego, CA, Apr. 1978, pp. 194–202.
[18] L. Accatino, G. Bertin, and M. Mongiardo, "A circular cavity structure for the efficient CAD of dual mode filters," in *IEEE MTT-S Int. Symp. Dig.*, San Francisco, CA, June 1996, pp. 1459–1462.

Luciano Accatino (M'84) was born in Turin, Italy, in 1950. He received the Doctor degree in electronic engineering from the Polytechnic of Turin, Turin, Italy, in 1973.

In 1975, he joined the Centro Studi e Laboratori, Telecomunicazioni (CSELT), Torino, Italy, where he was first engaged in the design of microstrip circuits and components. In 1980, he became involved in the design and development of microwave cavity filters and, subsequently, of various components for beam-forming networks. He then supervised the activities related to filters and waveguide components at CSELT stimulating a wide application of electromagnetic models to the design of all passive components. He has been the Head of the Microwave Department since 1994.

Giorgio Bertin (M'92) was born in Aosta, Italy, in 1956. He received the Doctor degree in electronic engineering from the Polytechnic of Turin, Turin, Italy, in 1982.

In 1983, he joined the Microwave Department, Centro Studi e Laboratori, Telecomunicazioni (CSELT), Torino, Italy, where he was first engaged in dielectric oscillator and dielectric-loaded cavity design. His activities then focused on the modeling of microwave discontinuities and the CAD of guiding structures, with particular attention devoted to discontinuities between nonstandard waveguides, such as those involving a dieletric loading or the presence of ridges. He is currently supervising all activities related to electromagnetic modeling.

Mauro Mongiardo (M'91) received the Laurea degree *summa cum laude* from the University of Rome, Rome, Italy, in 1983, and the Ph.D. degree from the University of Bath, Bath, U.K., in 1991.

He is currently an Associate Professor at the University of Perugia, Perugina, Italy. He has been Visiting Scientist at the University of Victoria, Victoria, B.C., Canada, the University of Bath, U.K., Oregon State University, Corvallis, and the Technical University, Munich, Germany. His main contributions are in the area of modeling of waveguide discontinuities, both in the cases of closed waveguides and open waveguides such as microstrip lines or coplanar waveguides. His research interests include numerical methods with contributions in the areas of mode-matching techniques, integral equations, variational techniques, FDTD, TLM, and FEM. He is also involved with frequency and time-domain analysis of MMIC's and is currently interested in the modeling and computer-aided procedures for the design of microwave and millimeter-wave components.